Earthquake Induced Damage Mitigation from Soil Liquefaction

CLASS A PREDICTION FOR LIQUEFACTION REMEDIATION INITIATIVE CENTRIFUGE TEST 4 (LRICT4)
(MITIGATION USING A DRAINAGE DYKE)

By:
Ahmad Jafari

Supervisor: Dr. Radu Popescu

Memorial University of Newfoundland

July 15, 2004

Introduction

In this report Class A prediction of the 4th LRI (Liquefaction Remediation Initiative) centrifuge test is presented and discussed. In this regard, the numerical model has been recalibrated based on the results of centrifuge tests LRICT2 and LRICT3, and used to perform Class A prediction for the fourth test.

Class A prediction of LRTCT1resulted in predicted slope displacements significantly larger than their recorded counterparts. Therefore, it was decided to recalibrate the numerical model using liquefaction strength data from the literature (Isotropically consolidated cyclic triaxial tests / Vaid et al. 2001).

Recalibration of the constitutive model

Recalibration of the numerical model has been done by curve fitting of the centrifuge data using the results of LRICT2 for reasonable ranges of soil parameters and liquefaction strength data mentioned earlier. Table 1 shows the selected values of the constitutive parameters based on class C predictions of LRICT2. This recalibration of the model based on the results of test 2 has been checked for test 3.

Constitutive parameters of Fraser River sand	**Symbol**	**Values**		**Type**
		Loose	**Dense**	
Mass density (kg/m^3) Porosity Hydraulic conductivity (permeability) (cm/s)	ρ_s n^w k	2710 0.448 0.0084	2710 0.406 0.0062	State Parameters
Low-strain shear modulus (Mpa) Reference effective mean normal stress Powe exponent Poisson ratio	G_0 p_0 n ν	45 100 0.5 0.3	78.3 100 0.5 0.3	Elastic Parameters
Friction angle at failure Coefficient of lateral earth pressure at rest Soil cohesion Maximum deviatoric strain (C= compression, E=extension)	ϕ k_0 c ε_{dev}^{max}	39^o 1 0 0.02 (C), 0.01 (E)	45^o 1 0 0.01 (C), 0.01 (E)	Yield Parameters
Dilation angle (phase transformation angle) Dilation parameter	ψ X_{PP}	34^o 0.27	34^o 0.05	Dilation Parameters

Table 1. New set of constitutive parameters from back analyses of tests 2 and 3 and used in class A prediction of test 4.

Importance of vertical motion

In all back analyses for tests 2 and 3, only the recorded horizontal input accelerations have been considered as input motions. In fact, no vertical acceleration was reported for test 2 and in case of test 3 the location of the measured vertical motion is not clear. Using the set of parameters listed in table 1, a numerical study was done for LRICT3 with both horizontal and vertical motion assuming that vertical motion is uniformly applied to the entire base of the model. Applying vertical motion resulted in significantly more dilative behavior for the slope compared to the case with no vertical input motion. Therefore, the new set of parameters listed in Table 1, may be on the stiff side if used with vertical motion. However, it was decided to use this set of parameters and no vertical motion in the numerical predictions due to the fact that vertical motion has not been recoded for all centrifuge tests (e.g. LRICT2), and distribution of the recorded vertical motion along the base of the centrifuge container is uncertain.

The results of back analyses of tests 2 and 3 will be submitted to place on the UBC website at a later time, and they will be discussed at the incoming meeting in Vancouver on August 4, 2004.

Effects of the coefficient of hydraulic conductivity

Comparison of the numerical results of LRICT2 with the corresponding recorded measurements at different pore pressure transducers indicates that dissipation of excess pore water pressure occurs faster in the numerical model compared to the relevant centrifuge experiment. This problem can be solved assuming lower values for the hydraulic conductivity of sand than those used in previous reports available on the UBC website at http://www.civil.ubc.ca/liquefaction/. The values, mentioned in Table 1 and used in class A prediction of LRICT4, are the reduced values of those used for previous class A predictions by a factor of 5.

LRICT4 geometry and input motion

General layout and input motion used for class A prediction of LRICT4 are similar to those of LRICT3 excepting the kind of dyke material. In LRICT4, dyke consists of drainage material instead of dense sand used in LRICT3. Figures 1 and 2 show the general layout and input acceleration used in class A prediction of LRICT4, respectively.

Soil properties of the drainage dyke

Regarding the drainage dyke, the following information, provided by C-CORE, is available, and used in the current class A prediction. No other information is available for soil properties of this dyke.

- Grain size distribution.
- Values of maximum and minimum void ratios, i.e., 0.81 and 0.62, respectively.
- Hydraulic conductivity (about 100 times higher than that of loose sand).
- Mass density (2670 kg/m^3).

Consequently, all soil parameters related to low-strain behavior, yield and dilation have been taken equal to those used for loose sand except for the friction angle, which was assumed to be $\varphi = 41^\circ$.

Results of Class A predictions for LRICT4

The following figures show the results of Class A prediction for LRICT4. As a general comment, the predicted displacements and settlements are very small, and slope is predicted to be stable. The predicted excess pore water pressure ratios inside dyke are very small due to the highly permeable material; however, in spite of the drainage dyke, liquefaction is predicted to occur in the free field upslope and at slope toe as illustrated in time histories of EPP2, EPP3, and EPP9. Also since reduced values for sand hydraulic conductivity are used for class A prediction, the predicted dissipation rate of pore water pressure is very slow. This can be seen in excess pore water pressure time histories at EPP2, EPP3, and EPP9 as well as in excess pore water pressure contours provided at different instants, i.e., figures 5 to 8.

References

Earthquake Induced Damage Mitigation from Soil Liquefaction website. 2003. Posted at: http://www.civil.ubc.ca/liquefaction/.

Vaid, Y.P., Stedman, J.D., and Sivathayalan, S. 2001. Confining stress and static shear effects in cyclic liquefaction. Can. Geotech. J. 38: 580-591.

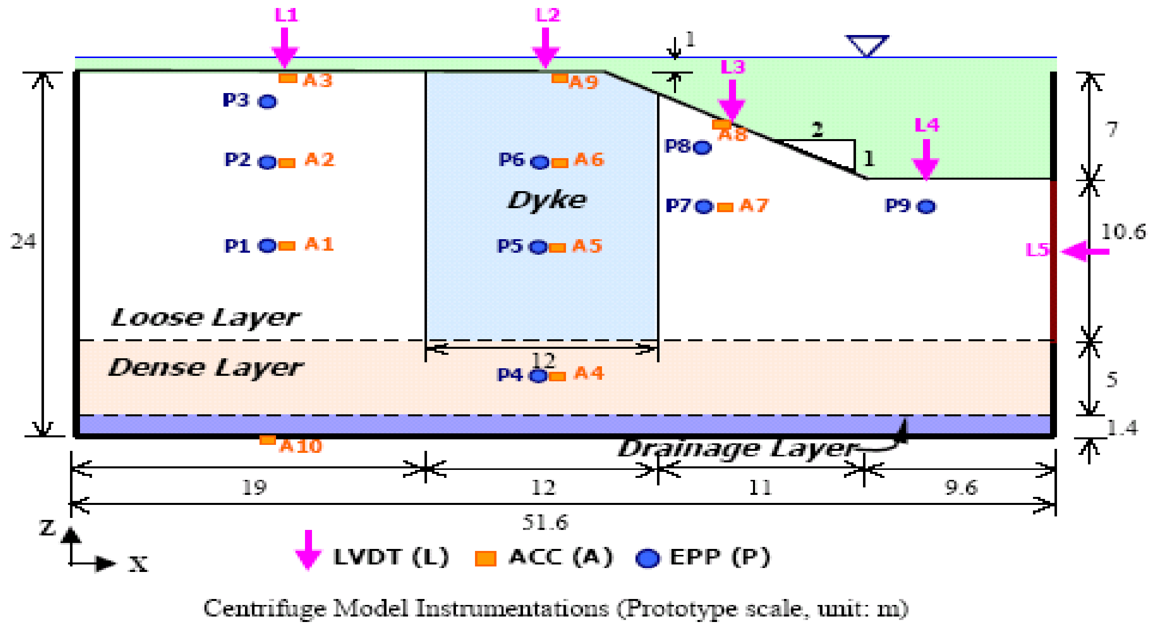

Figure 1. General layout of LRI centrifuge tests (From UBC website)
(The slope is improved by a drainage dyke in LRICT4.)

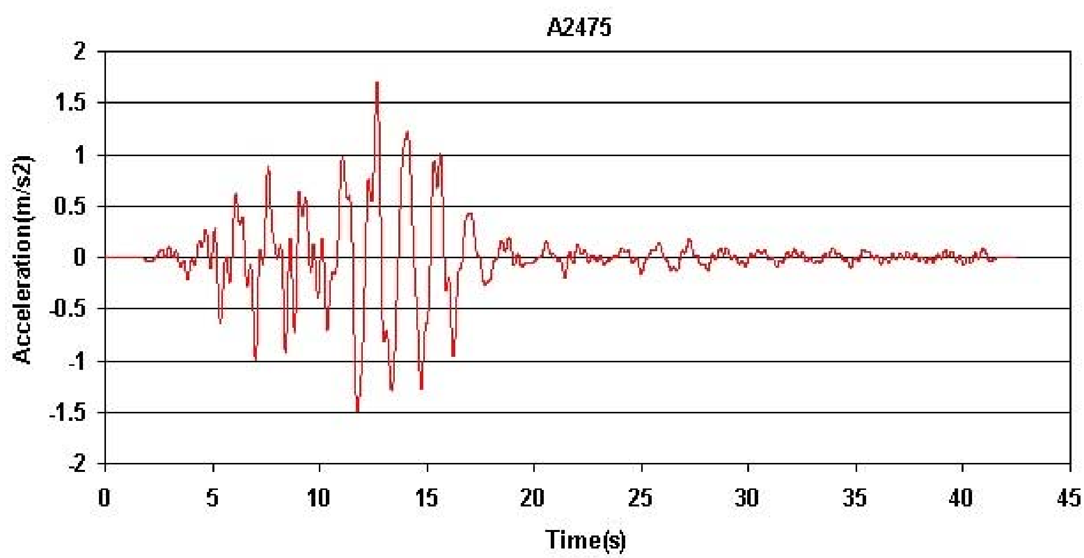

Figure 2. Input acceleration time history
(Data from UBC website)

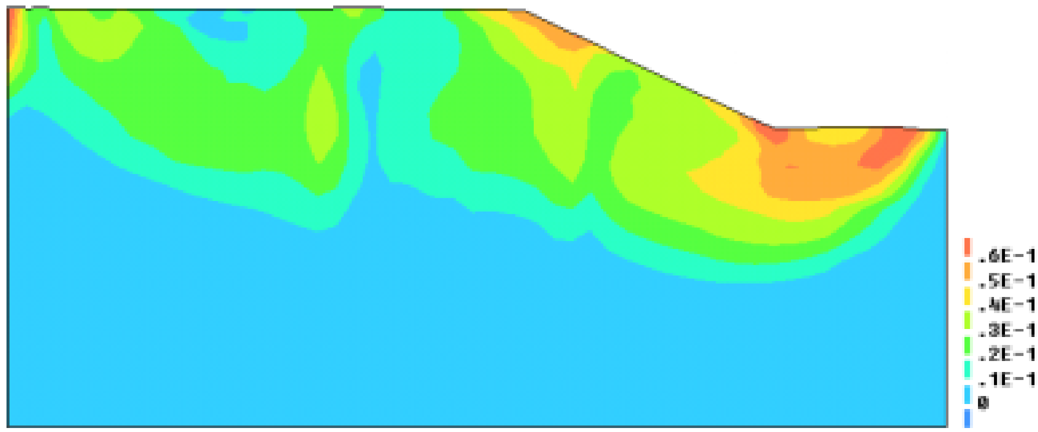

Figure 3. Predicted maximum shear strain contours at the end of analysis (t=42.6 s) (Deformation magnification factor=1)

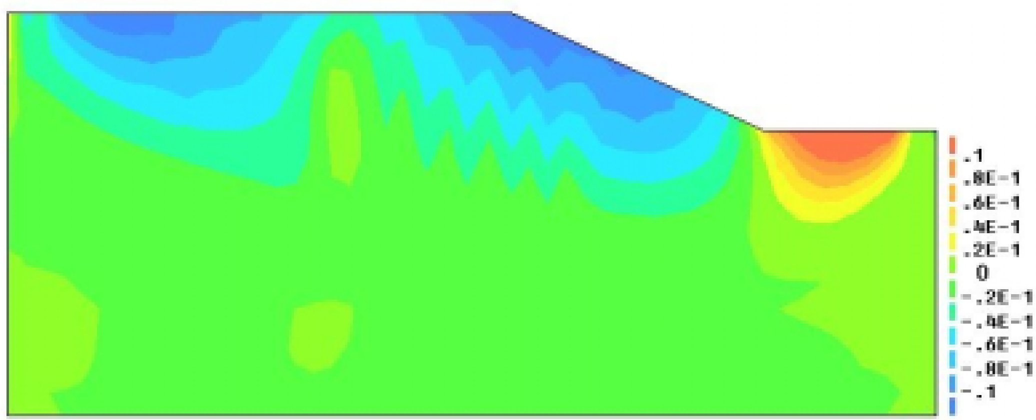

Figure 4. Predicted vertical displacement contours at the end of analysis (t=42.6 s)

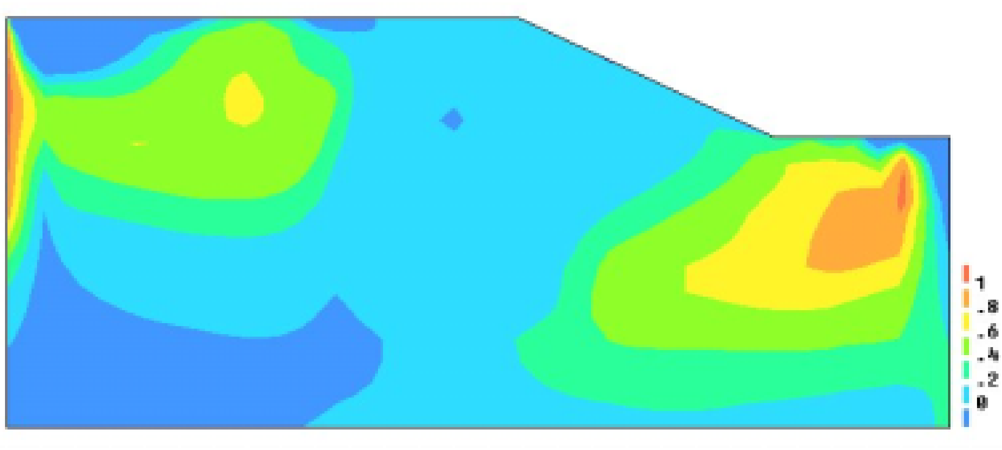

Figure 5. Predicted excess pore water pressure contours at t= 12 s

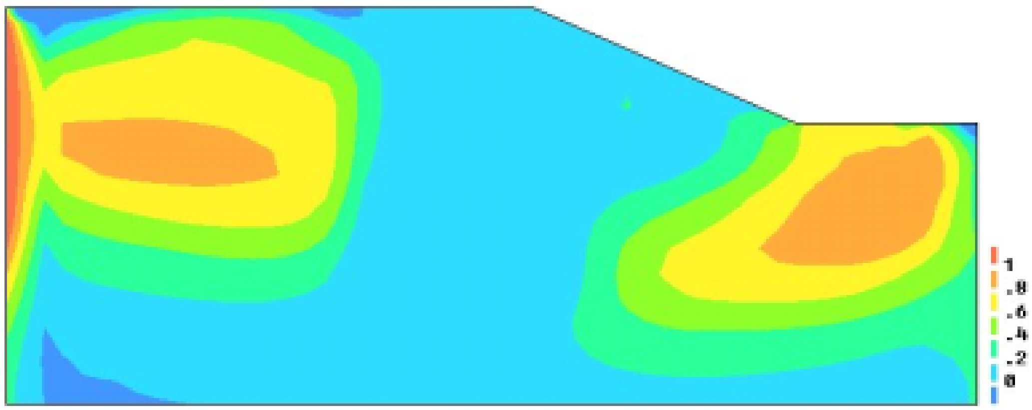

Figure 6. Predicted excess pore water pressure contours at t= 16 s

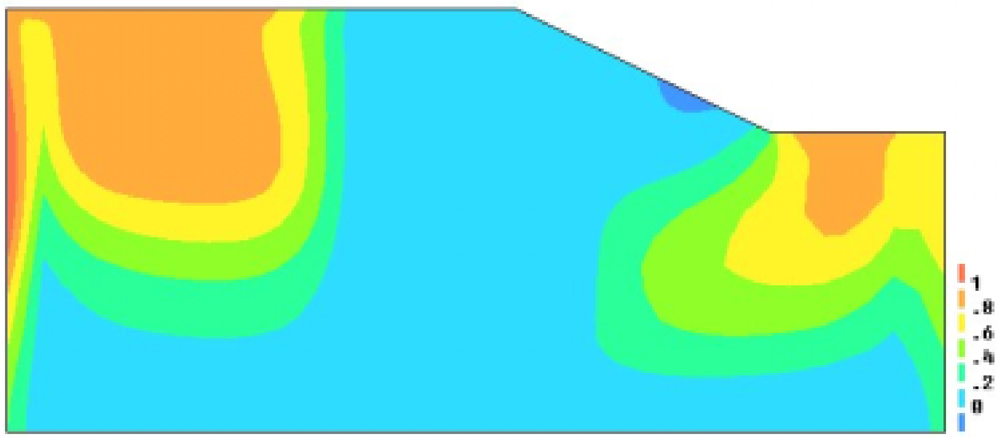

Figure 7. Predicted excess pore water pressure contours at t= 20 s

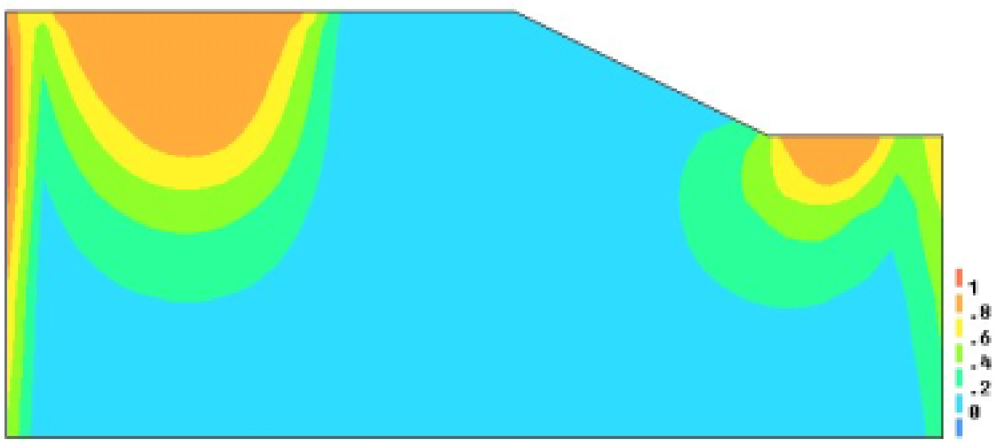

Figure 8. Predicted excess pore water pressure contours at t= 42.6 s

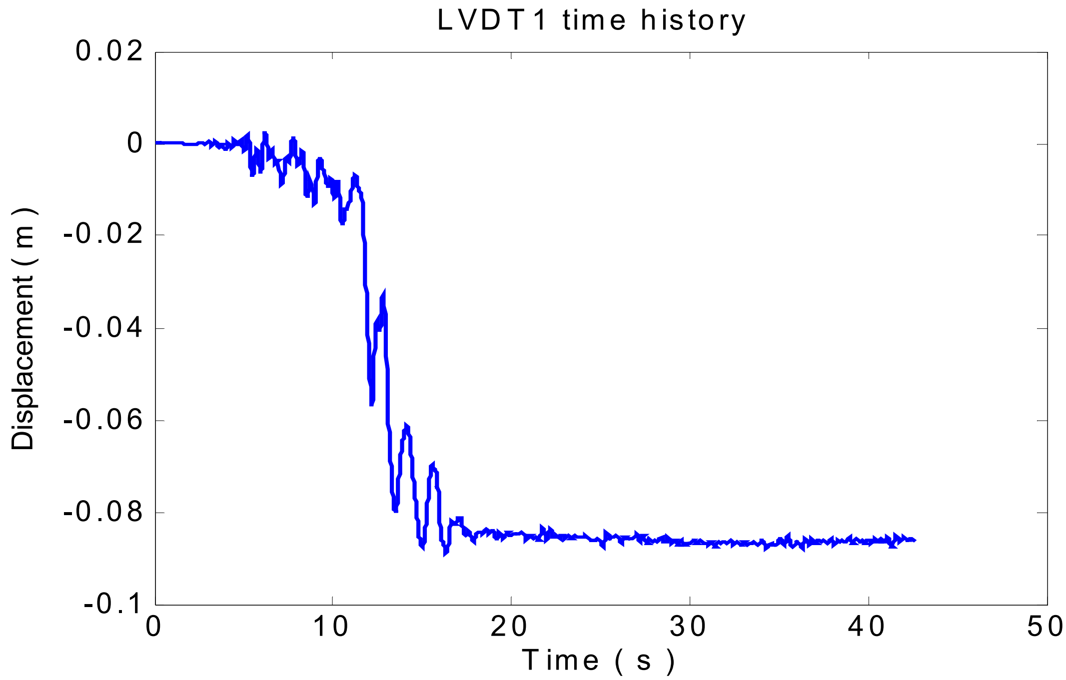

Figure 9. Predicted vertical displacement time history at LVDT1

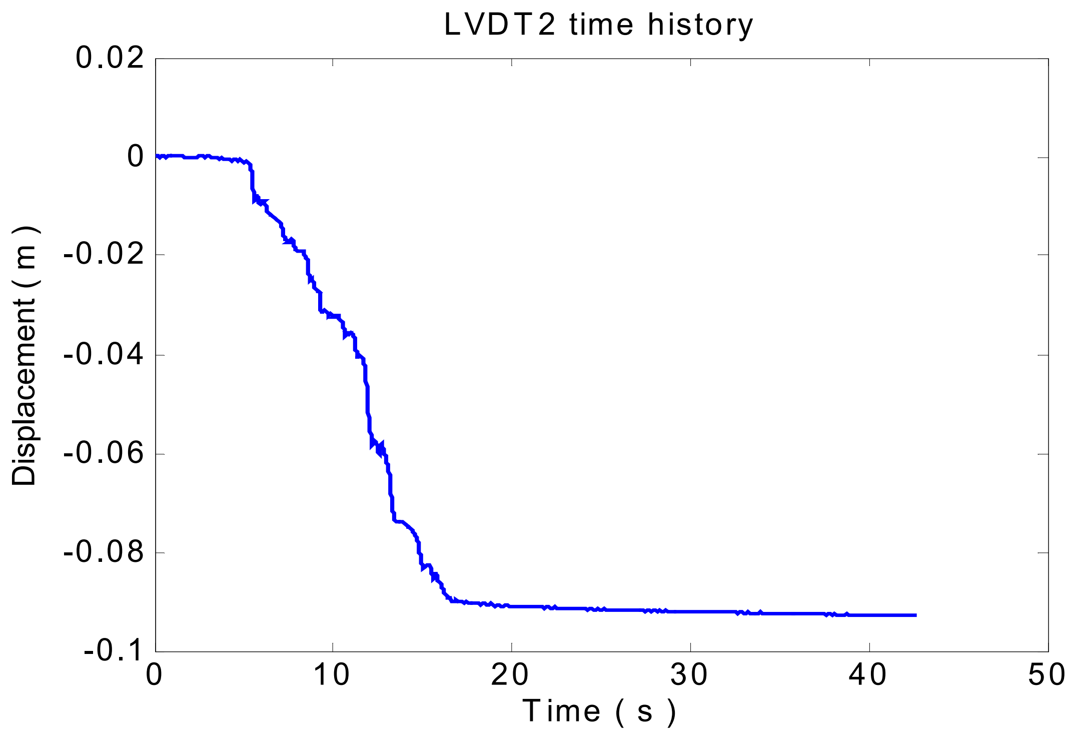

Figure 10. Predicted vertical displacement time history at LVDT2

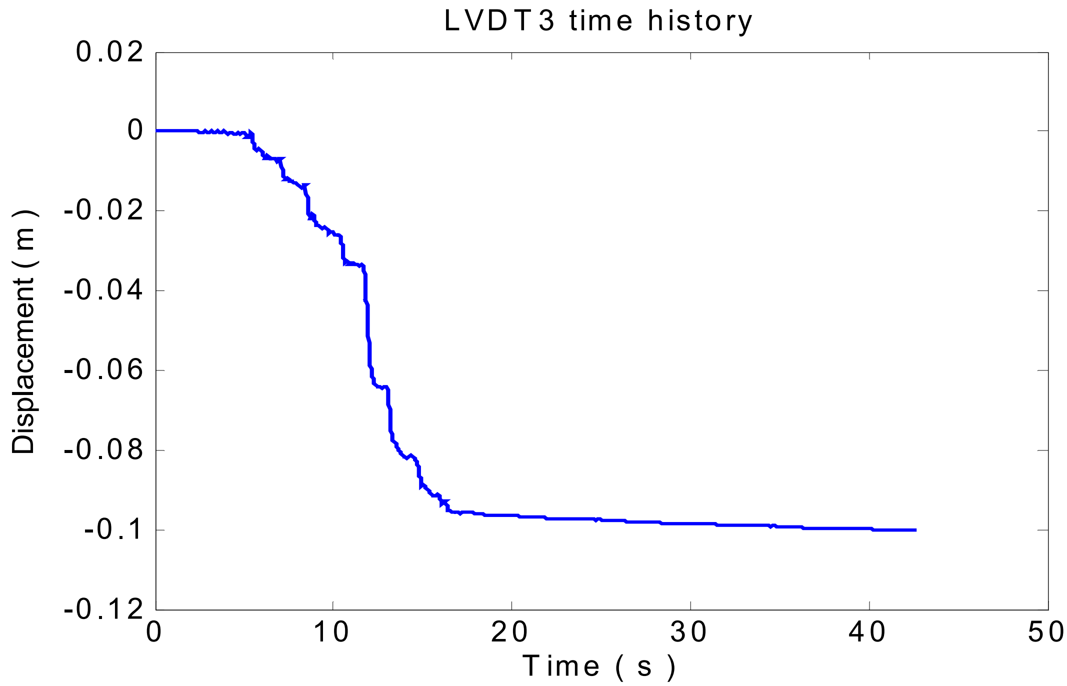

Figure 11. Predicted vertical displacement time history at LVDT3

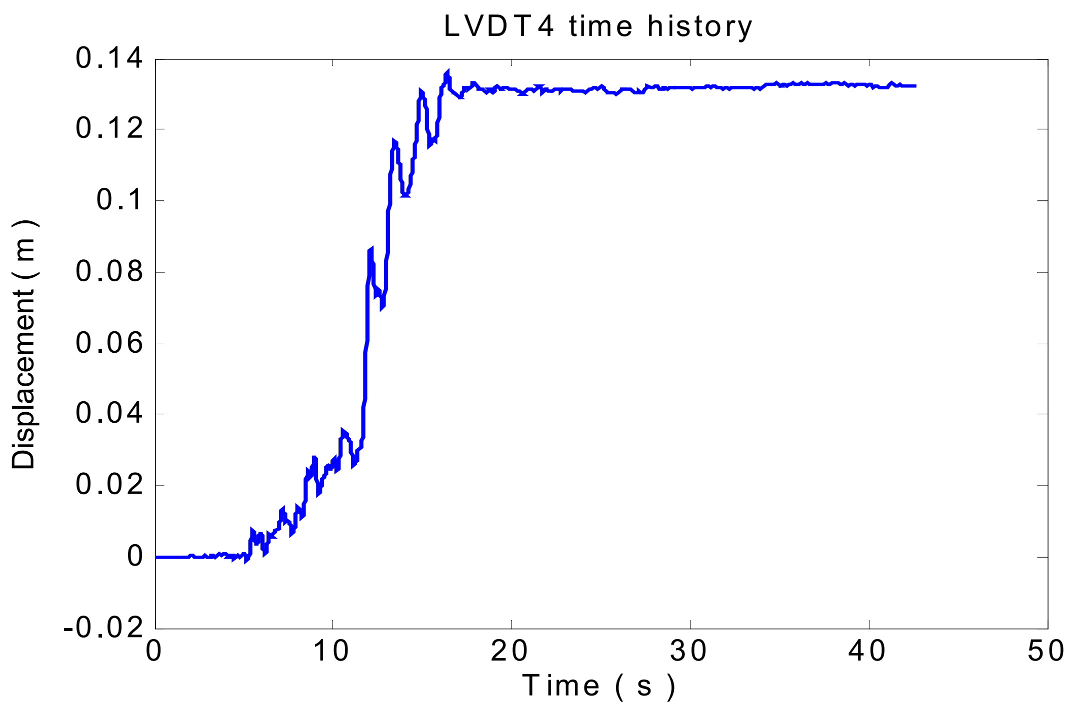

Figure 12. Predicted vertical displacement time history at LVDT4

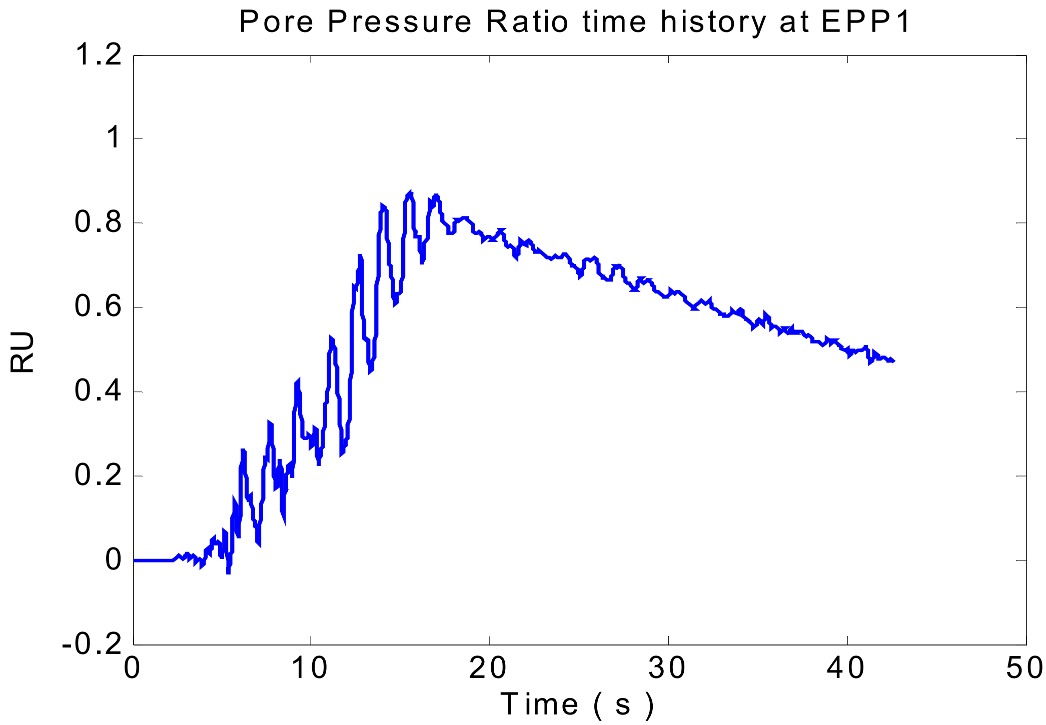

Figure 13. Predicted excess pore water pressure ratio time history at EPP1.
(Initial effective vertical stress = 107 KPa)

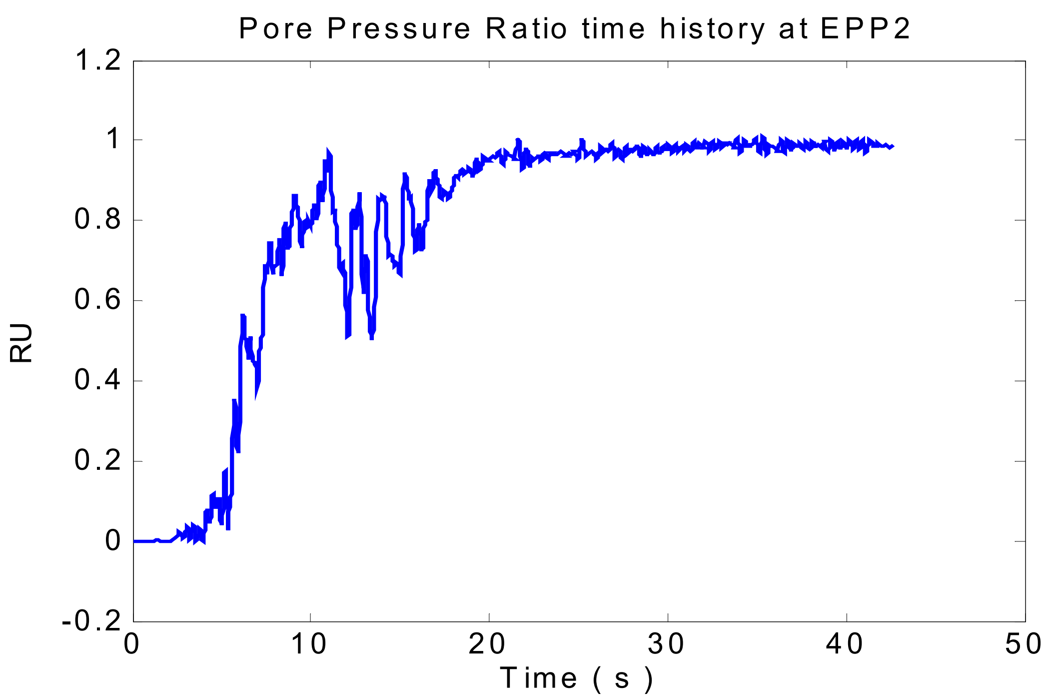

Figure 14. Predicted excess pore water pressure ratio time history at EPP2.
(Initial effective vertical stress = 56 KPa)

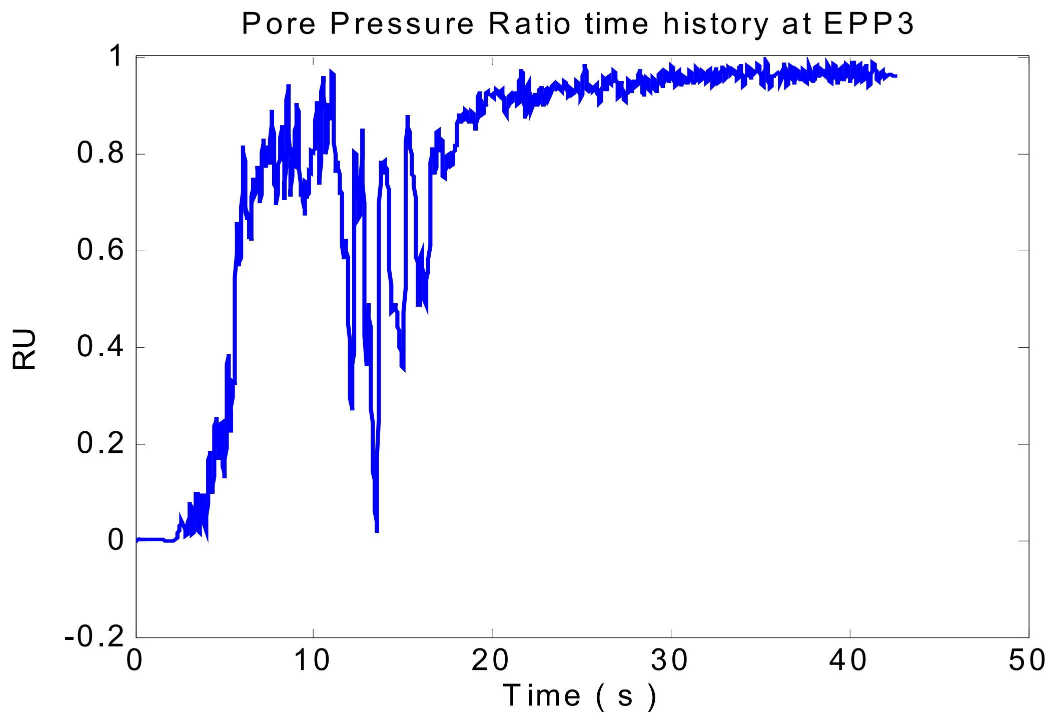

Figure 15 Predicted excess pore water pressure ratio time history at EPP3.
(Initial effective vertical stress = 20 KPa)

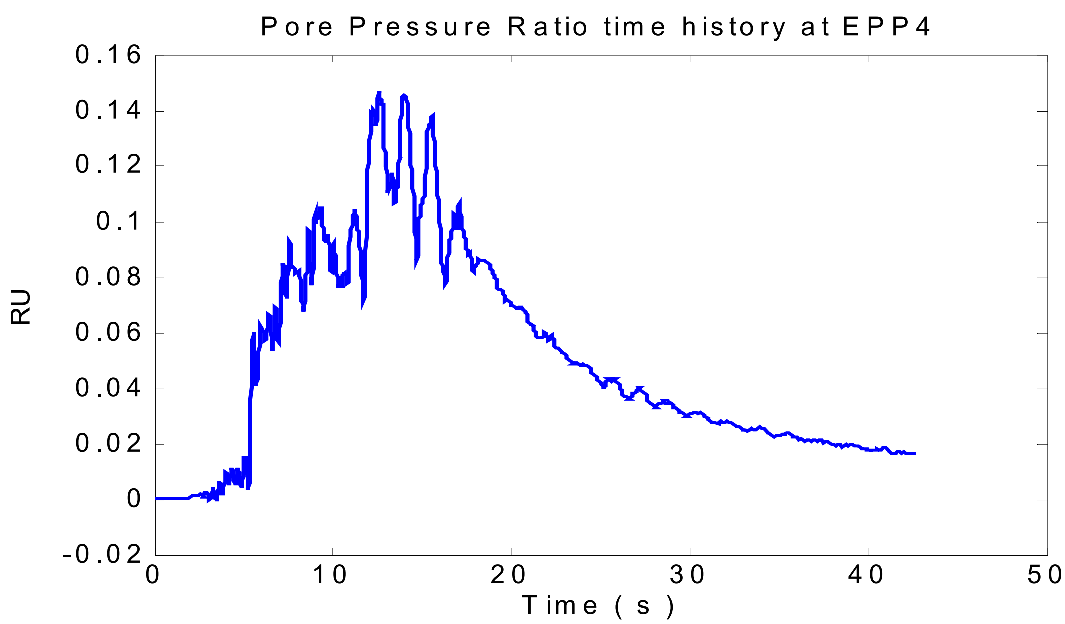

Figure 16. Predicted excess pore water pressure ratio time history at EPP4.
(Initial effective vertical stress = 180 KPa)

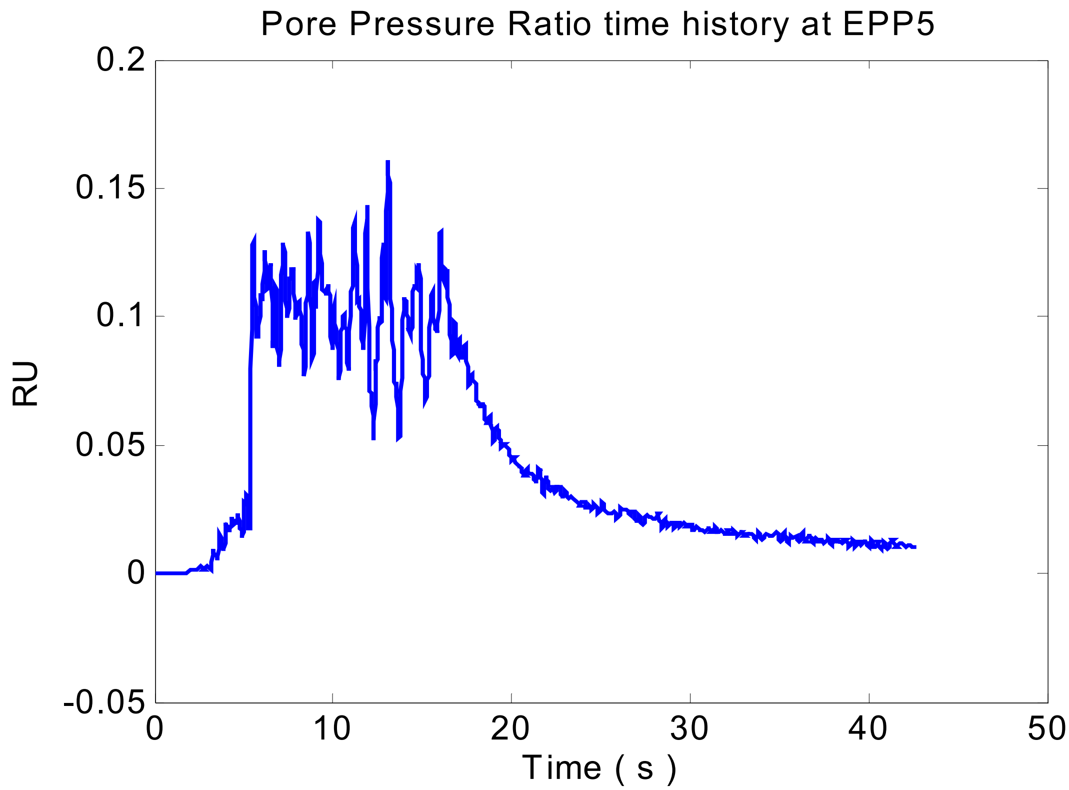

Figure 17. Predicted excess pore water pressure ratio time history at EPP5.
(Initial effective vertical stress = 103.5 KPa)

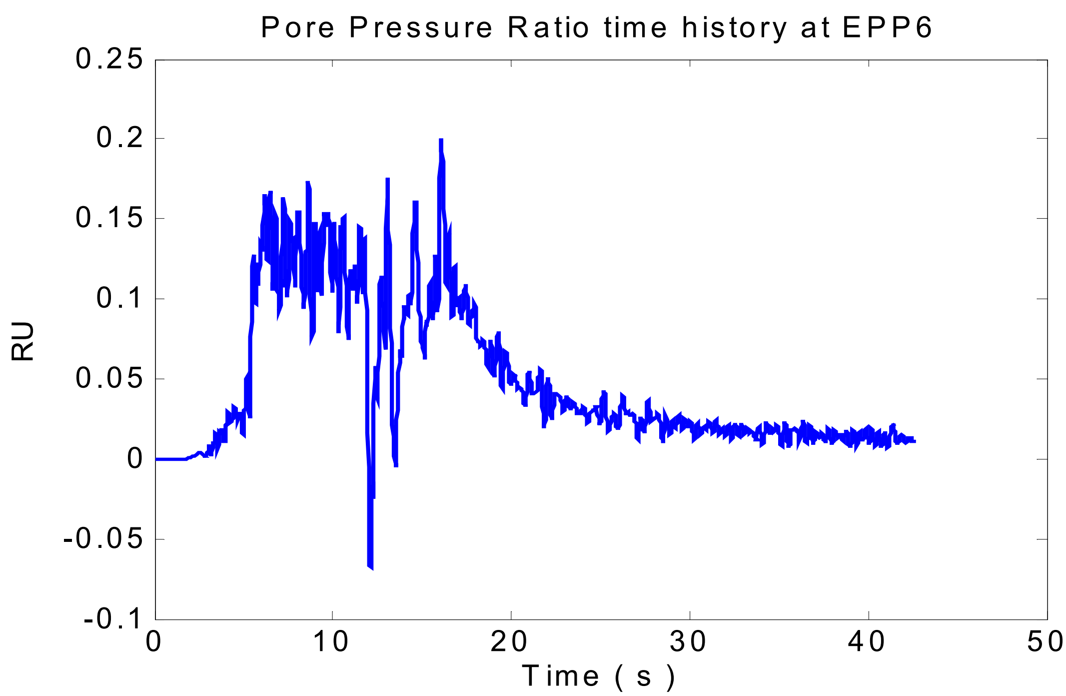

Figure 18. Predicted excess pore water pressure ratio time history at EPP6.
(Initial effective vertical stress = 55 KPa)

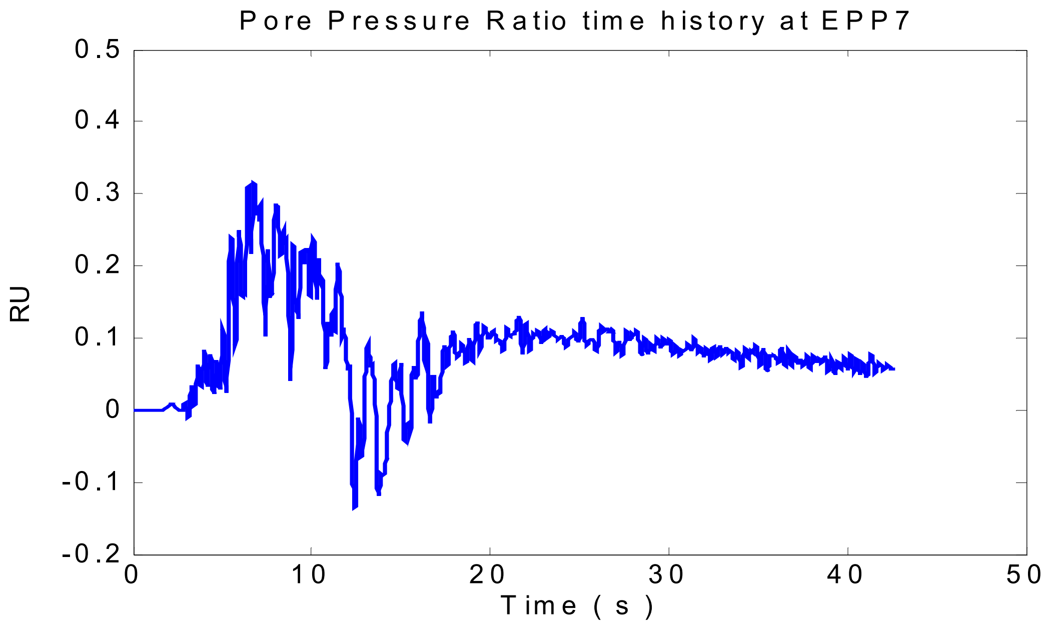

Figure 19. Predicted excess pore water pressure ratio time history at EPP7.
(Initial effective vertical stress = 60 KPa)

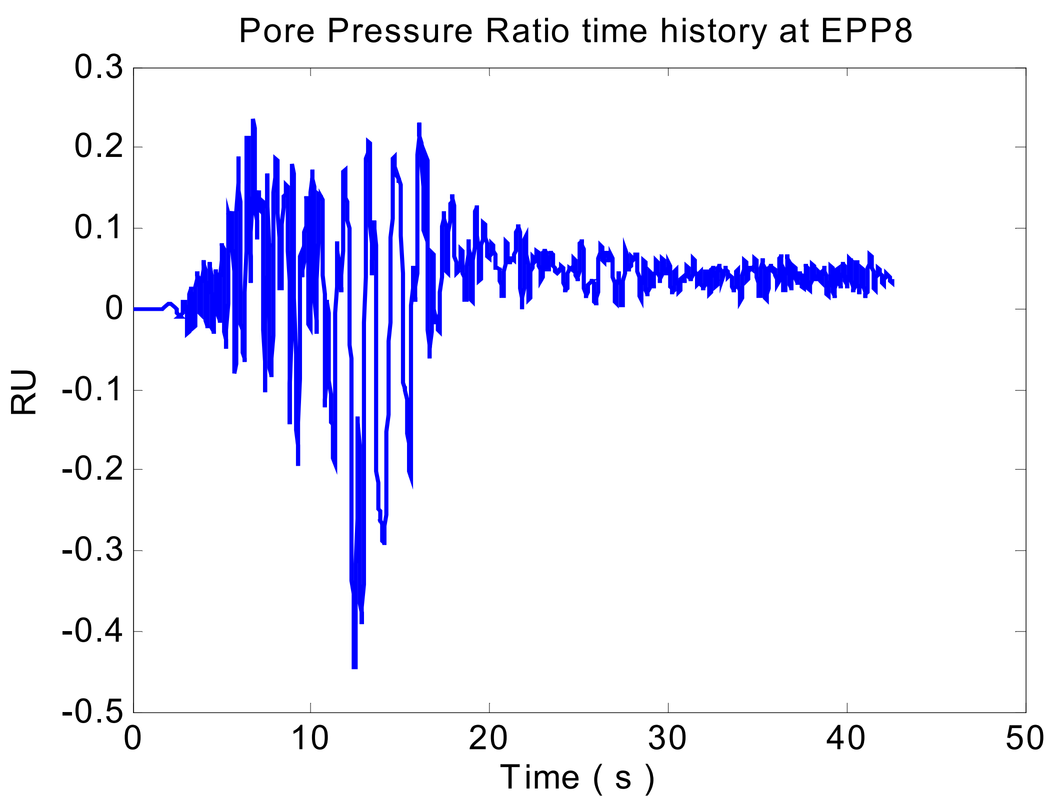

Figure 20 Predicted excess pore water pressure ratio time history at EPP8.
(Initial effective vertical stress = 26 KPa)

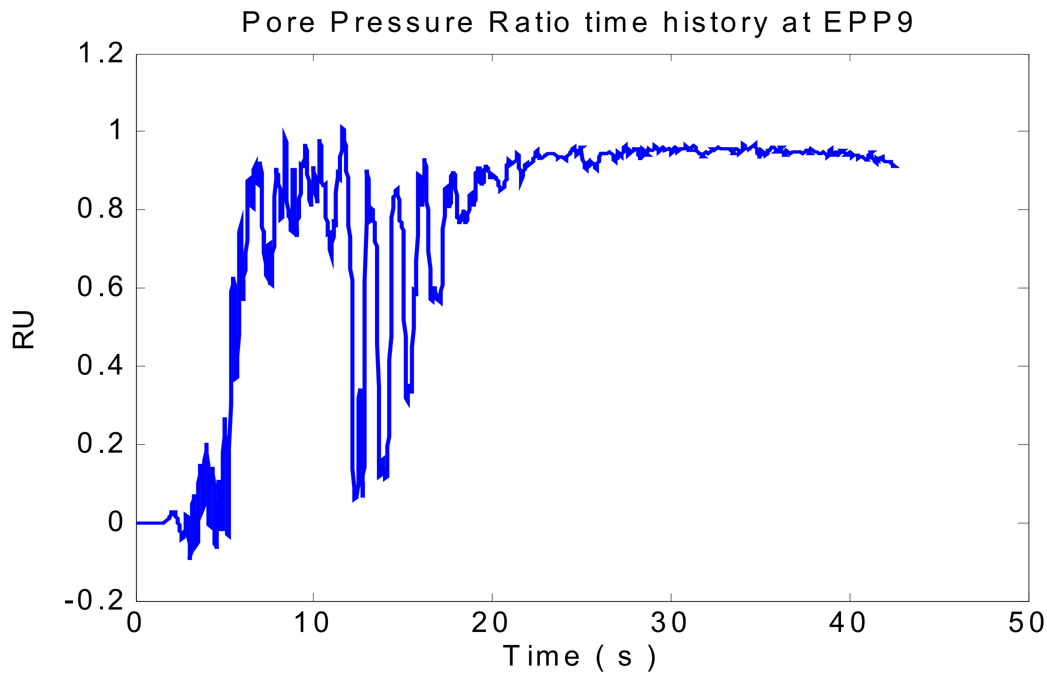

Figure 21. Predicted excess pore water pressure ratio time history at EPP9.
(Initial effective vertical stress = 20 KPa)

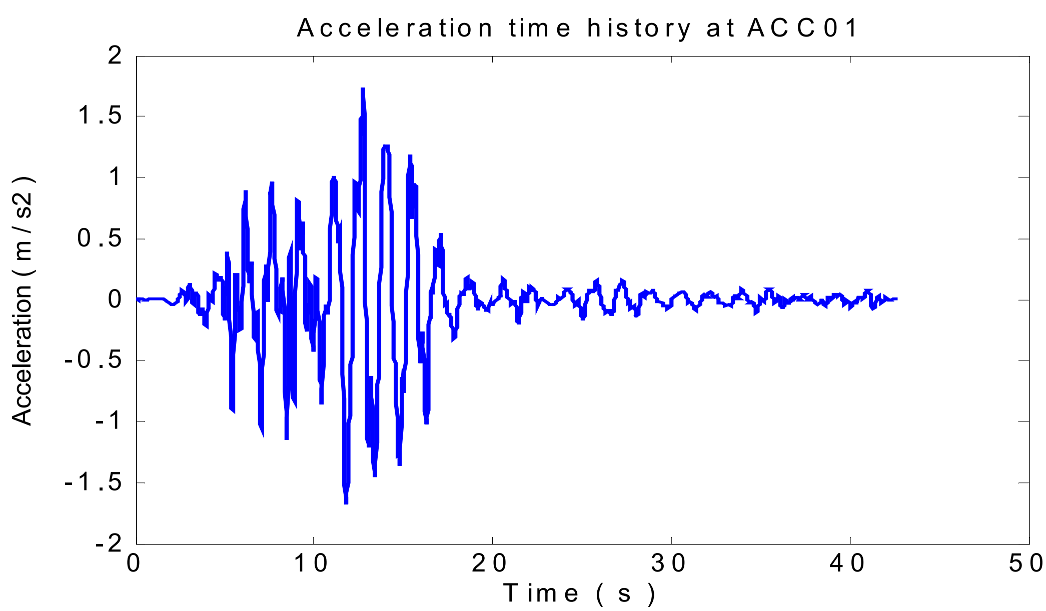

Figure 22. Predicted acceleration time history at ACC01.

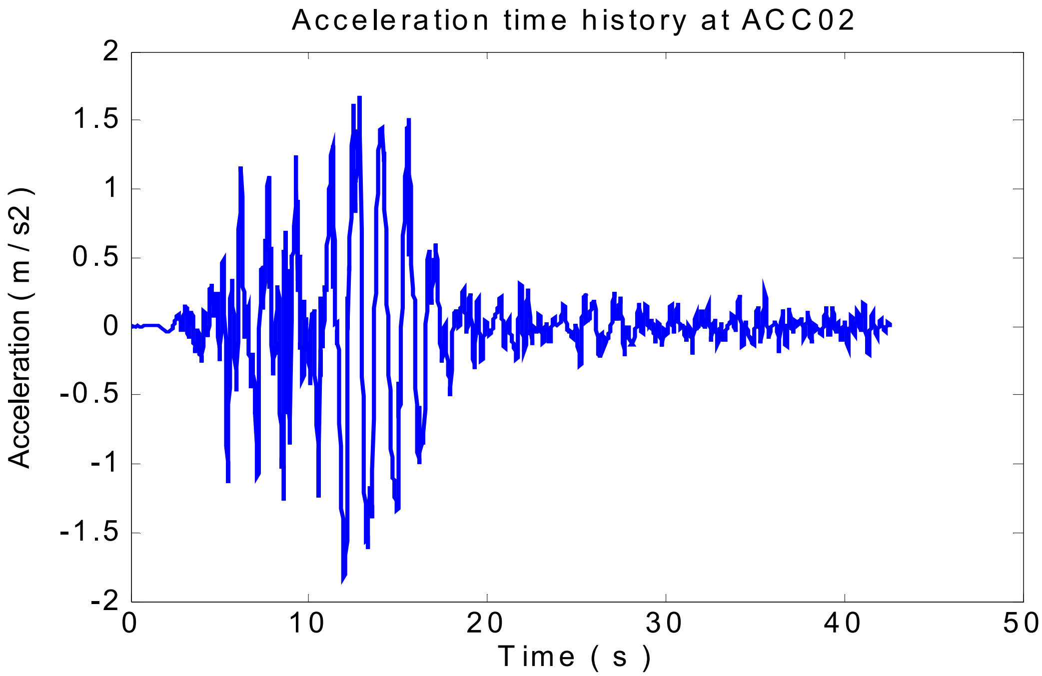

Figure 23 Predicted acceleration time history at ACC02.

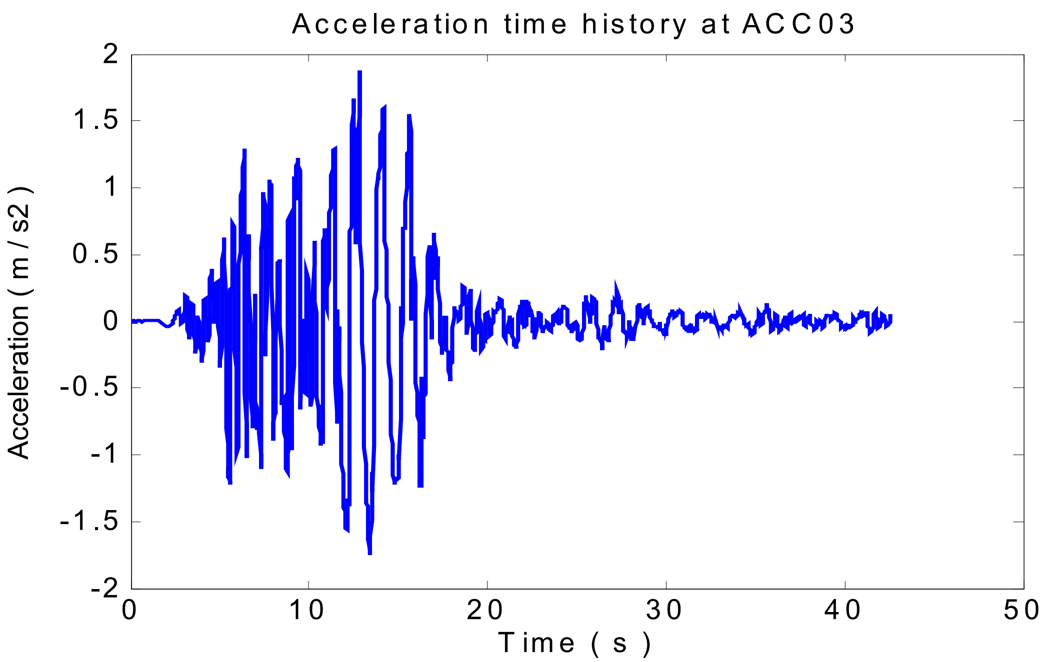

Figure 24 Predicted acceleration time history at ACC03.

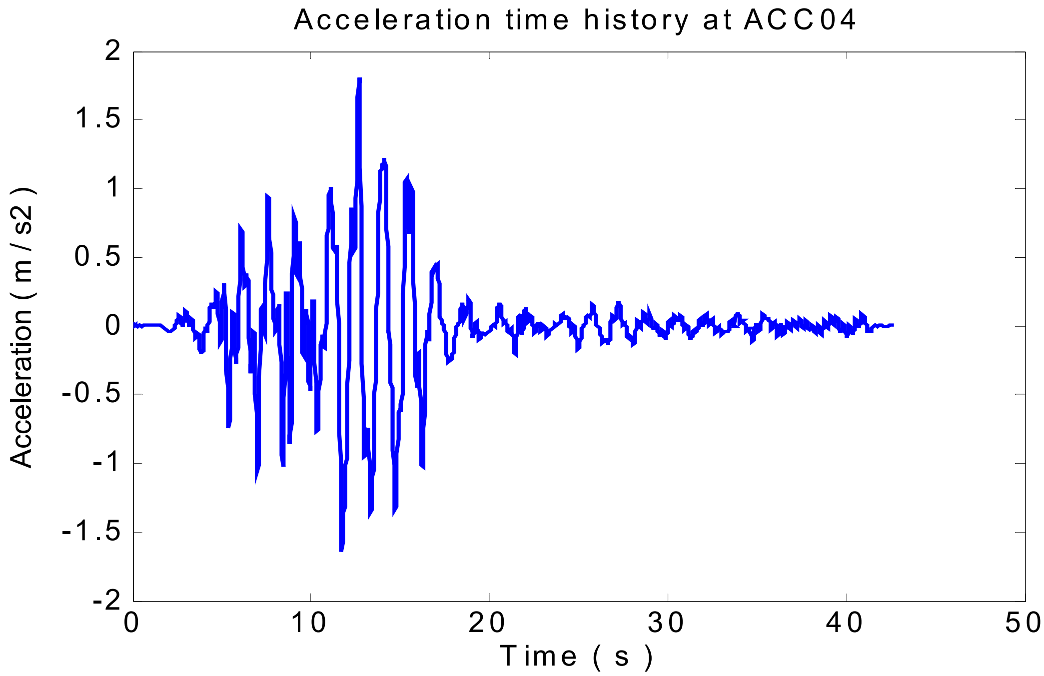

Figure 25 Predicted acceleration time history at ACC04.

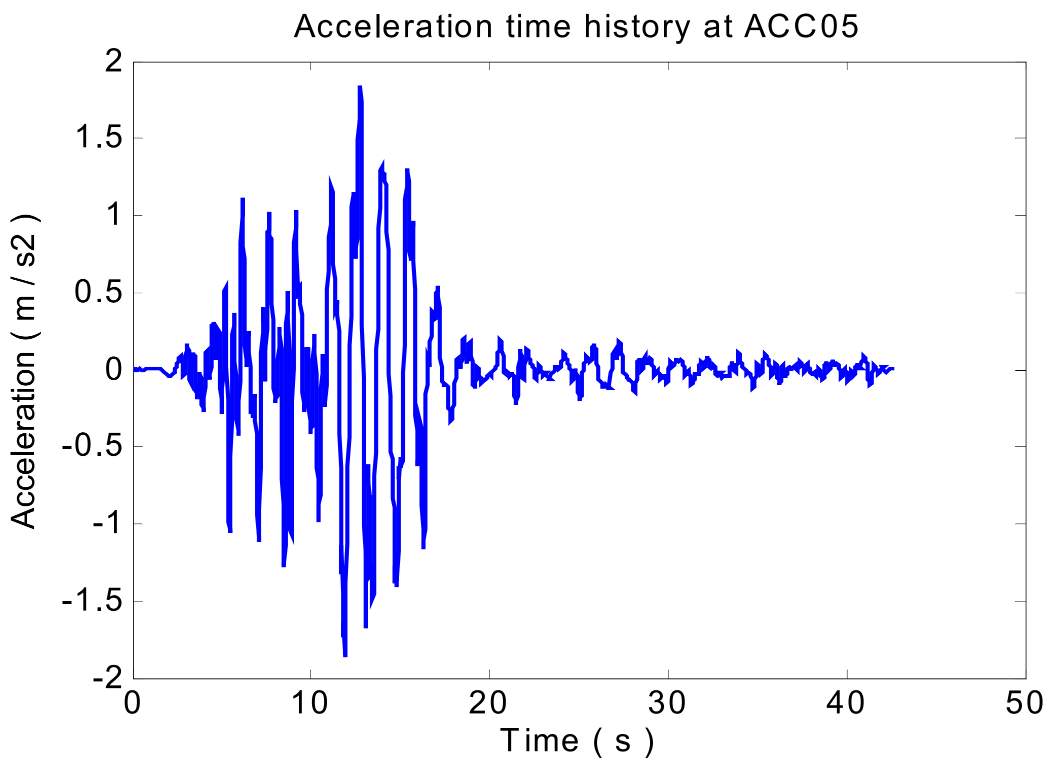

Figure 26 Predicted acceleration time history at ACC05.

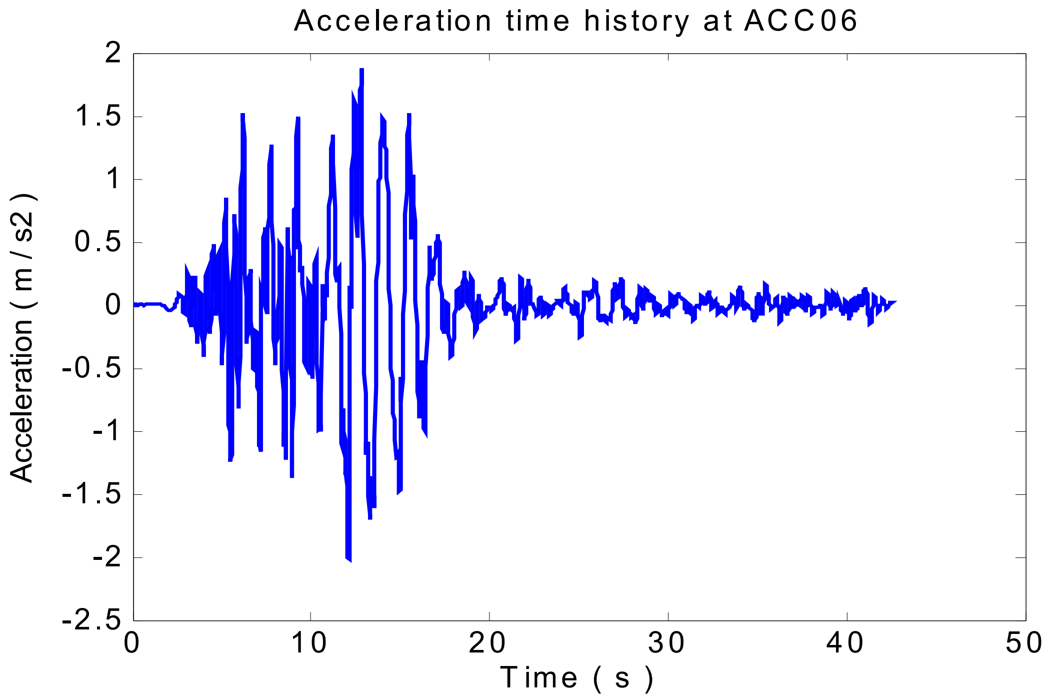

Figure 27 Predicted acceleration time history at ACC06.

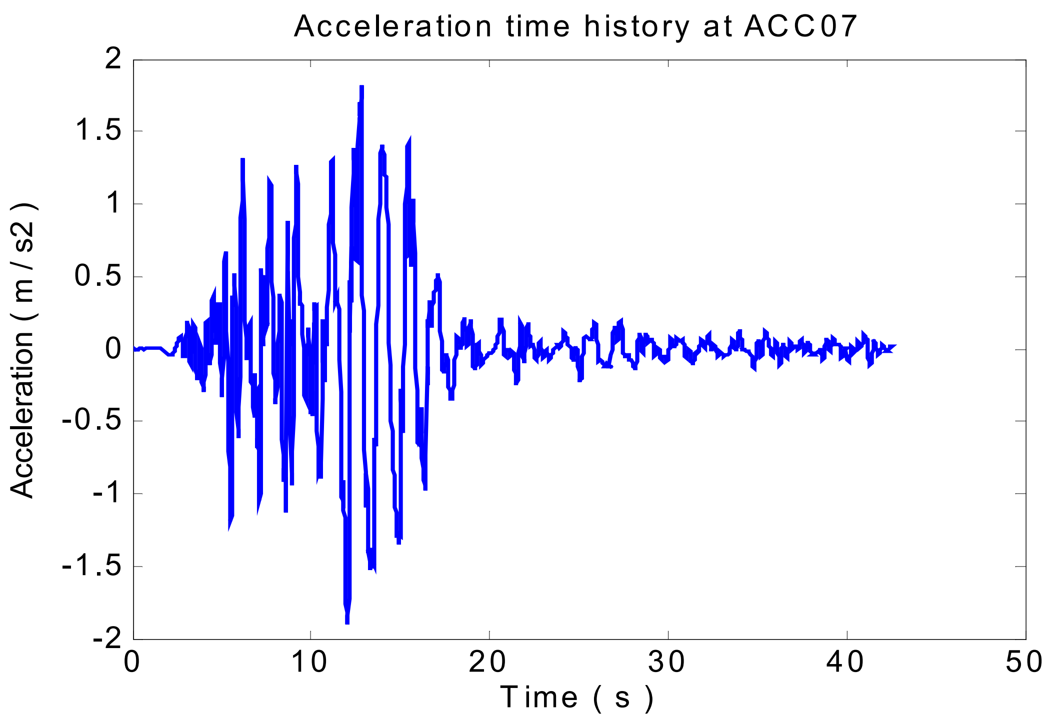

Figure 28 Predicted acceleration time history at ACC07.

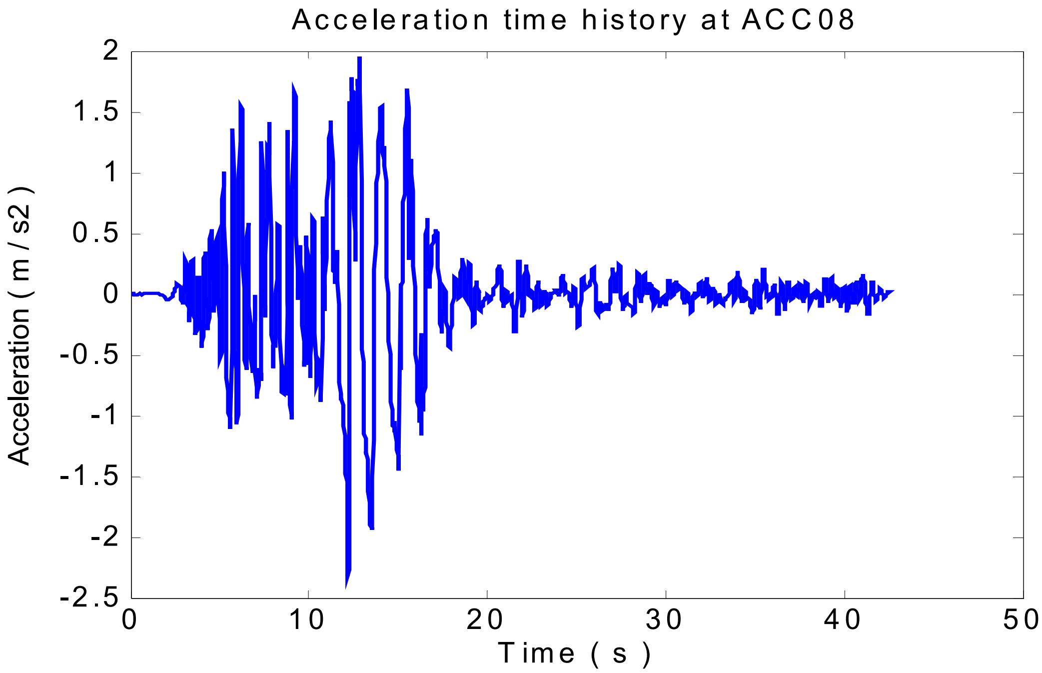

Figure 29 Predicted acceleration time history at ACC08.

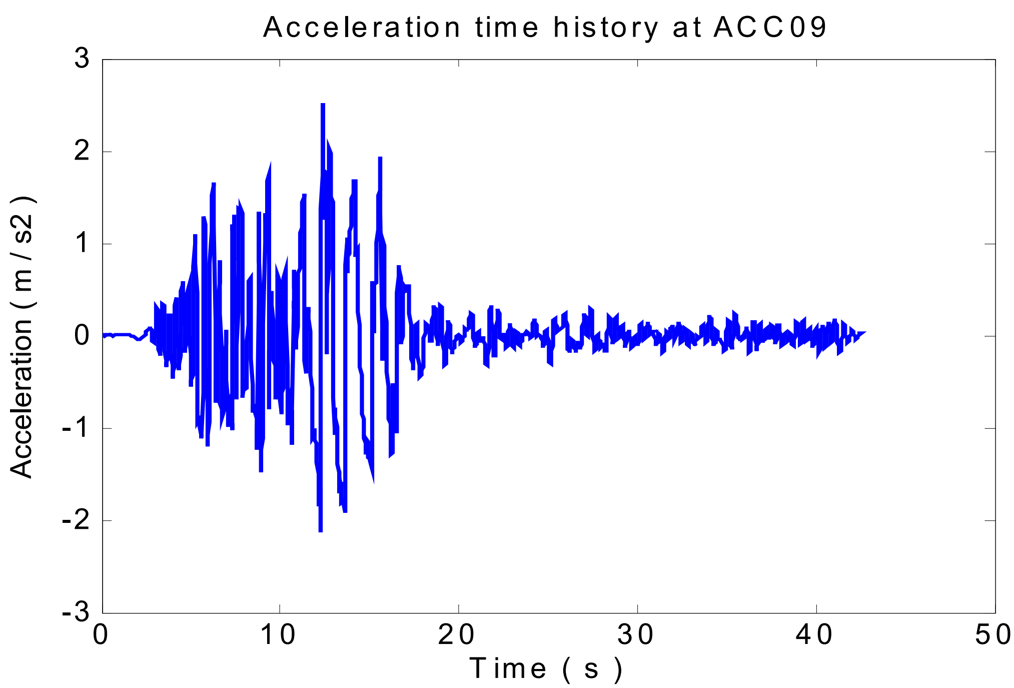

Figure 30 Predicted acceleration time history at ACC09.